

# Three-dimensional (3D) reconstruction and quantitative analysis of the microvasculature in medulloblastoma and ependymoma subtypes

H. Jacobus Gilhuis · Jeroen A. W. M. van der Laak · Jacqueline Pomp ·  
Arnoud C. Kappelle · Johanna M. M. Gijtenbeek · Pieter Wesseling

Received: 8 March 2006 / Accepted: 5 September 2006 / Published online: 16 November 2006  
© Springer Science+Business Media B.V. 2006

**Abstract** In the World Health Organisation (WHO) classification of tumours of the nervous system, four main histopathological subtypes of medulloblastomas (classic medulloblastoma, desmoplastic medulloblastoma, medulloblastoma with extensive nodularity and advanced neuronal differentiation and large cell/anaplastic medulloblastoma) as well as of ependymal tumours (low-grade ependymoma, anaplastic ependymoma, myxopapillary ependymoma and subependymoma) are recognised. Under the hypothesis that the microvascular architecture of tumours is a reflection of the histopathological subtype, we performed three-dimensional reconstructions of the microvasculature in these subtypes of medulloblastomas and ependymal tumours using computerised image analysis. In addition, we quantitatively assessed three microvascular parameters (number, area, perimeter) in these neoplasms. Three-dimensional reconstructions showed a dense pattern of irregular vessels in classic and large cell medulloblastoma. In desmoplastic medulloblastoma and medulloblastoma with extensive

nodularity, the vessels were more unevenly distributed and organised around the nodular areas. Classic medulloblastoma and large cell medulloblastoma had on average the largest vessel area and perimeter. The highest number of vessels was seen in classic medulloblastoma and medulloblastoma with extensive nodularity. Three-dimensional analysis of ependymal tumours showed that low-grade ependymoma had larger but fewer vessels compared to anaplastic ependymoma, while myxopapillary ependymoma had a complex, heterogeneous pattern of vessels and subependymoma few but regular vessels. In ependymal tumours, the highest values for vessel number, vessel area and vessel perimeter were found in anaplastic ependymoma and the lowest values in subependymoma. We conclude that our three-dimensional reconstructions shed unprecedented light on the tumour vasculature in medulloblastomas and ependymal tumours and expect that such reconstructions are helpful tools for further studies on tumour angiogenesis.

**Keywords** Angiogenesis · Ependymoma · Medulloblastoma · Three-dimensional reconstructions · Vasculature

H. J. Gilhuis (✉) · A. C. Kappelle ·  
J. M. M. Gijtenbeek

Department of Neurology, Radboud University Nijmegen  
Medical Centre, P.O. Box 9101, 6500 HB, Nijmegen,  
The Netherlands  
e-mail: gilhuis@rdgg.nl

J. A. W. M. van der Laak · P. Wesseling  
Department of Pathology, Radboud University Nijmegen  
Medical Centre, P.O. Box 9101, 6500 HB, Nijmegen,  
The Netherlands

J. Pomp  
Department of Radiotherapy, Reinier de Graaf Hospital,  
P.O. Box 5011, 2625 AD Delft, The Netherlands

## Introduction

Medulloblastomas (MBs) and intracranial ependymal tumours (ETs) are neuroepithelial tumours, mainly occurring in individuals younger than 16 years old. Spinal ETs occur in all age groups [1–3]. The World Health Organisation (WHO) classification of tumours of the nervous system distinguishes four main histo-

pathological subtypes of MBs and of ETs. MB variants are classic MB, desmoplastic MB, MB with extensive nodularity and advanced neuronal differentiation and large cell/anaplastic MB. ET variants are low-grade ependymoma (lgE; WHO grade II), anaplastic ependymoma (aE; WHO grade III), myxopapillary ependymoma (mpE; WHO grade I) and subependymoma (subE; WHO grade I) [3]. The MB subtypes mentioned above are all designated by the WHO as high-grade (grade IV) malignancies and so far are considered as belonging to the same spectrum. In the ET group, on the other hand, subE and mpE are different entities rather than belonging to the spectrum of lgE and aE.

Treatment for MBs and intracranial lgEs and aEs is not yet based on histopathological features. However, some recent studies show that children with a large cell/anaplastic MB have a poorer outcome [4, 5], whereas children with a MB with extensive nodularity tend to fare better than children with other MB subtypes [6]. The prognostic significance of histological malignancy grade in lgEs and aEs is unclear [3]. MpEs generally have an indolent behaviour and do not need additional therapy after gross total resection. SubEs are often coincidental findings during autopsy and only sporadically cause clinical symptoms [3, 7].

There is a huge interest in the tumour vasculature as a potential target for anti-tumour therapy [8–10]. So far, knowledge about the tumour microvasculature in MBs and ETs is limited. Accurate visualisation of the microvascular network is important for a better understanding of tumour angiogenesis. We therefore performed three-dimensional (3D) reconstruction as well as quantitative analysis of three vascular parameters (number, area, perimeter) in the main histopathological subtypes of MBs and ETs under the hypothesis that the histopathological subtype is reflected by the microvascular architecture. For 3D reconstruction, a recently developed technique was applied [11]. The 3D images of the tumour microvasculature were compared to those of normal cerebral neocortex, cerebral white matter and cerebellar cortex and white matter.

## Materials and methods

### Tissues

Representative biopsy samples of a paraffin embedded classic MB, desmoplastic MB, MB with extensive nodularity, large cell MB, supratentorial lgE, posterior fossa aE, spinal mpE and supratentorial subE, as well as autopsy material of adult normal cerebral neocortex, cerebral white matter, cerebellar cortex and cerebellar white matter were selected from the archives of the

Department of Pathology, Radboud University Nijmegen Medical Centre. A special method was used to allow for cutting up to 60 serial sections of constant thickness and with minimal loss or distortion of tissue [11]. For 3D visualisation in this study, we investigated 45–60 serial 4 µm sections. The serial sections were stained for endothelial cells with a monoclonal antibody to CD34 (mouse monoclonal, 1:750, Neomarkers, Fremont, USA). Immunostaining was performed using the avidin–biotin-complex method; the chromagen used to highlight vessels was 3,3'- Diaminebenzidine tetrahydrochloride (DAB), resulting in a brown product. Separate CD34-positive structures were considered as separate microvascular structures. In order to improve the signal to noise ratio during image acquisition, no counterstaining was used.

### 3D visualisation

Computerised 3D visualisation of the vascular bed was performed as recently described by our group [11]. In short, 45–60 images of corresponding microscopic fields in subsequent tissue sections were digitally stored. A microscopic field (10 × objective, field size 0.74 mm<sup>2</sup>) was aligned as closely as possible with a rotating microscope stage, using an image overlay on the computer screen depicting the vascular profiles of the previous tissue section. After storage of an entire series of images, automated recognition of vascular profiles (image segmentation) was performed based on positive immunohistochemical staining of endothelial cells. Results of segmentation for each microscopic field were shown as an overlay in the original image on a computer screen for visual inspection and if necessary, interactive correction. Image registration was fine-tuned automatically using an affine image transformer, which corrects for shifts, rotations and stretching in *x* and *y* direction. Finally, 3D visualisation was performed using a marching cube algorithm, resulting in static images of the 3D reconstruction. Of each tumour, two representative microscopic areas were analysed in this way. Cerebral neocortex, cerebral white matter, cerebellar cortex and cerebellar white matter of a normal human brain obtained by autopsy, served as control tissues.

### Quantitative analysis of vasculature

Quantitative analysis of the vasculature was performed for each tumour in a single tissue section halfway the series of CD34-stained serial sections according to the method we described earlier [12]. In addition, the same was done on normal cerebellar and cerebral cortex and white matter. In the section used for quantitative

analysis 8–20 microscopic fields ( $10\times$  objective, field size  $0.74\text{ mm}^2$ ) were analysed and in these fields the vessel number, area and perimeter were calculated.

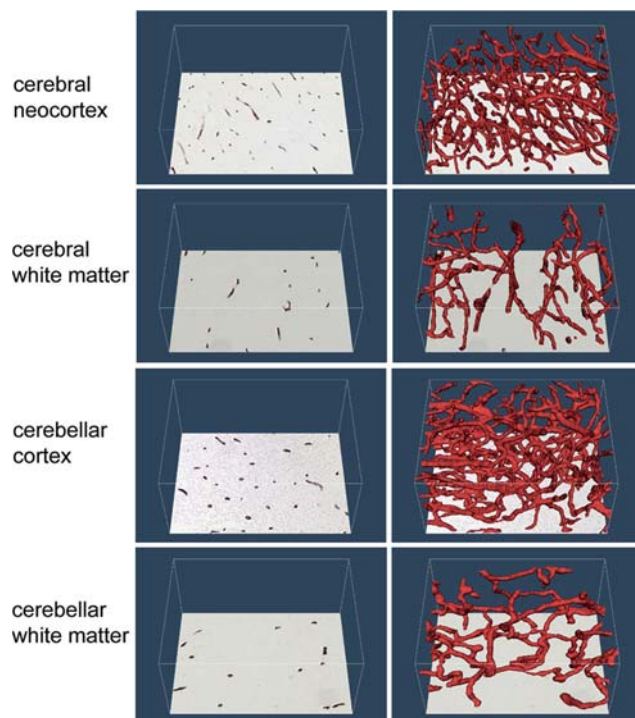
## Results

Figure 1 shows a compilation of haematoxylin and eosin (H&E) stained sections (first row), CD34 stained areas highlighting the tumour vasculature (second and fourth row) and 3D reconstructions of the microvasculature in these areas (third and fifth row) in four subtypes of MB and ET. For comparison, similar images of normal cerebral neocortex, cerebral white matter, cerebellar cortex, and cerebellar white matter are included. Figures of normal cerebral neocortex and white matter were obtained with kind permission from Gijtenbeek et al. [11]. Figure 2 shows the results of quantitative assessment of vessel number, area, perimeter and diameter of the cerebral neocortex, cerebral white matter, cerebellar cortex and cerebellar

white matter and of the MB and ET subtypes, that were used for 3D reconstruction of the microvasculature.

### Normal cerebral and cerebellar tissue

3D reconstruction of the cerebral neocortex, cerebral white matter, cerebellar cortex and cerebellar white matter revealed a regular vascular pattern with little variation in the vessel diameter. Compared to normal cerebral and cerebellar white matter, the cerebral neocortex and the cerebellar cortex had a more intense, somewhat more delicate, but regular vascular pattern (Fig. 1). The microvascular parameters in cerebral neocortex and cerebellar cortex were in the same range for vessel area and perimeter, while vessel number was higher in cerebellar cortex. Compared to normal cerebral and cerebellar white matter, these parameters in cerebral neocortex and cerebellar cortex were more variable. In cerebral and cerebellar white matter the vessel number, area and perimeter were comparable and relatively low, with little variation from field to field (Fig. 2).



**Fig. 1** Haematoxylin and eosin (H&E) stained histological sections (original magnification  $\times 100$ ), two-dimensional images (immunohistochemical (CD34) staining for endothelial cells) and 3D reconstructions of the vasculature of cerebral neocortex, cerebral white matter, cerebellar cortex, cerebellar white matter, classic MB, desmoplastic MB, MB with extensive nodularity, large cell MB, supratentorial IgE, posterior fossa aE, spinal mPE, and supratentorial subE. The arrows in the H&E stained sections of desmoplastic MB and MB with extensive nodularity indicate nodular ('pale island') zones.

### MBs

With 3D reconstruction, classic MB had a dense, more or less evenly distributed microvascular pattern, the vessels showing a variable diameter. In desmoplastic and extensive nodularity MBs, the blood vessels showed an uneven distribution with organisation around the nodular ('pale island') zones. Large cell MB blood vessels showed an uneven distribution and the formation of tufts. Compared to normal cerebellar cortex and white matter (i.e. the tissue in which MBs occur), more variation was present for all microvascular parameters in all MB subtypes. However, the values for the parameters were generally still in the range of normal cerebellar cortex or white matter. In occasional microscopic fields, the vessel number in large cell MB was lower than in normal cerebellar white matter, while in some fields the vessel area and vessel perimeter in classic and large cell MB exceeded those of normal cerebellar cortex. Median vessel area and perimeter were higher in classic and large cell MB than in desmoplastic and extensive nodularity MB, while median vessel number were higher for classic and extensive nodularity MB. Variation for vessel area and perimeter was most extensive in classic and large cell MB. Variation for vessel number was largest in classic MB and MB with extensive nodularity.



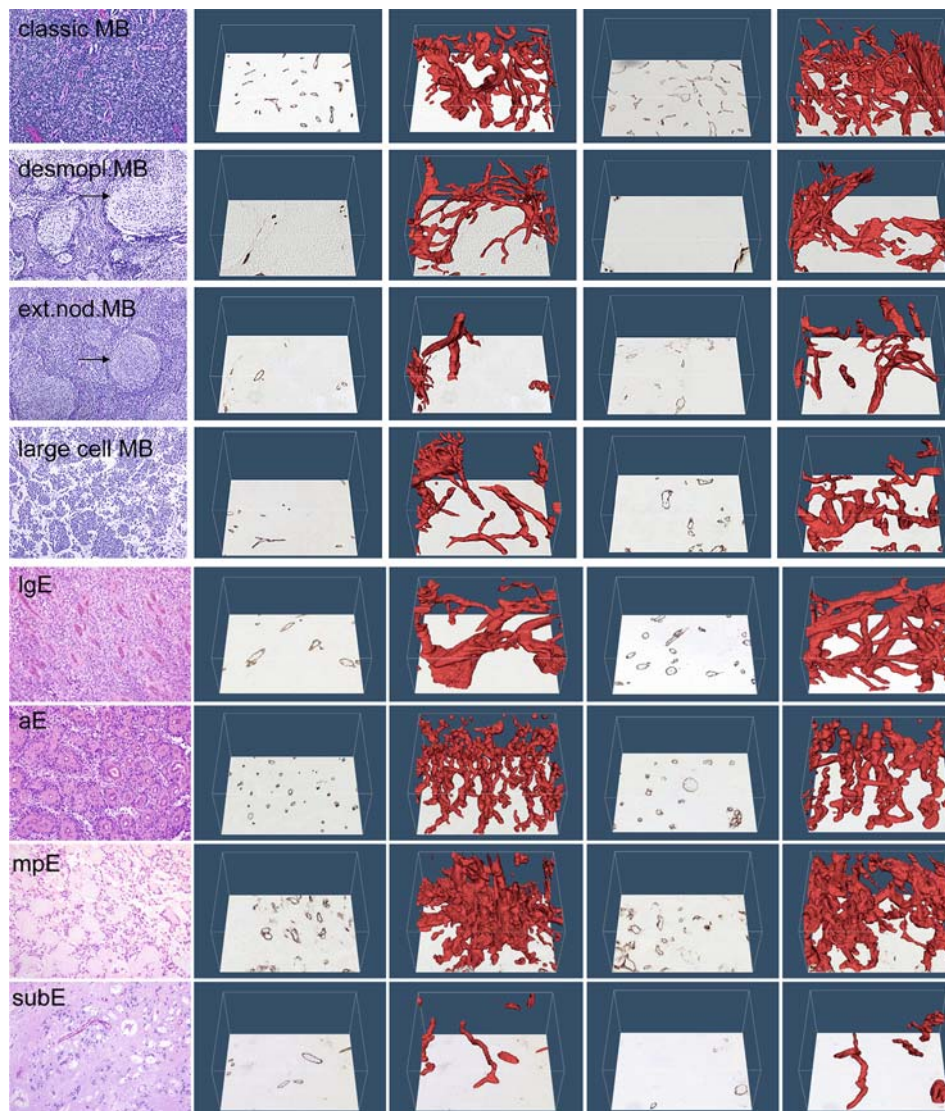


**Fig. 1** continued

## ETs

3D reconstructions of the ETs showed that IgE had fewer but larger vessels as compared to aE. MpE contained a complex, irregular and partly dense vascular pattern, while subE showed relatively few but regular vessels. The vascular parameters in low grade and anaplastic ET were comparable, showed much more variation than in normal cerebral and cerebellar tissue and while vessel number and perimeter were in the range of normal brain tissue, the vessel area was found to be much higher. In contrast, in subE all three vascular parameters were lower than in normal cerebral and cerebellar white matter. The mpE showed a relatively high variation for vascular parameters over the different fields, in some of them the values for these parameters were in the range of subE, while in

others the value for vascular area and perimeter (but not for vessel number) exceeded that of normal cerebral neocortex and cerebellar cortex.

## Discussion

Studies on angiogenesis in tumours of the CNS generally focussed on astroglial tumours (for recent review, see [10]) and relatively little attention has been given to this process in MBs and ETs. Some studies in the latter tumours investigated angiogenesis as a prognostic factor for survival, or as a possible target for therapy [13–18]. Thus far, the correlation between survival and vascular pattern is unclear for MBs and ETs. In a study of 23 patients with MBs, Ozer et al. [16] found high vessel density to be a significant unfavourable

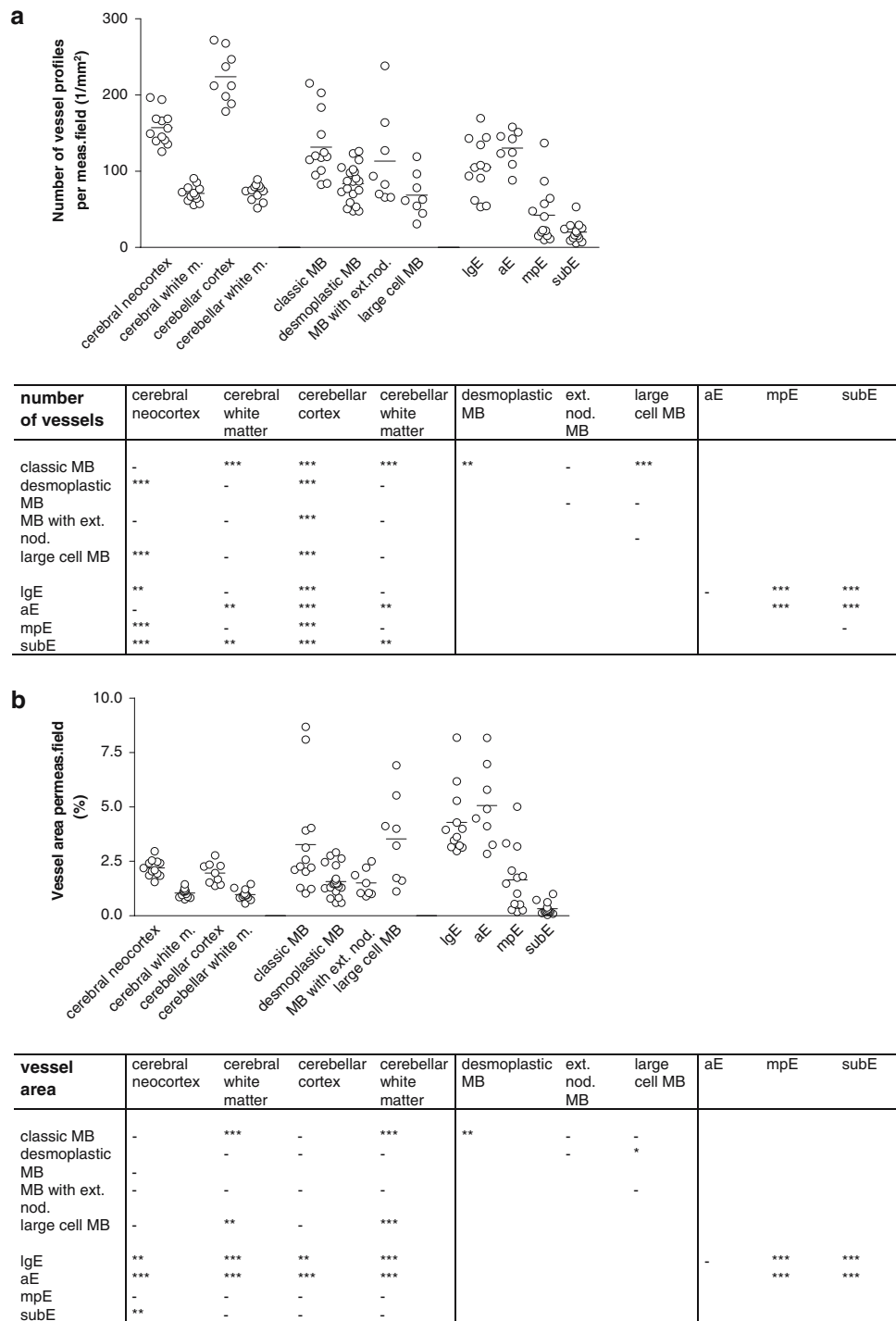


**Fig. 2** Results of quantitative analysis of vessel number (a) area; (b) perimeter; (c) of cerebral neocortex, cerebral white matter, cerebellar cortex, cerebellar white matter, classic MB, desmoplastic MB, MB with extensive nodularity, large cell MB, supratentorial IgE, posterior fossa aE, spinal mpE, supratentorial subE. Vessel number—number of complete vascular profiles in a field; each vascular profile demarcated from the surrounding tissue by the immuno-histochemical (CD34) staining for endothelial cells was considered as a separate blood vessel. Vessel

number is the vascular density of the field; vessel area the sum of areas of all individual vascular profiles in a field in  $\mu\text{m}^2$ ; vessel perimeter the sum of perimeters of all individual vascular profiles in a field in  $\mu\text{m}$  [11]. Horizontal line indicates mean. Each circle represents one measured field. Abbreviations; ext. nod. = extensive nodularity, m. = matter, meas. = measured. Statistical analysis (anova test), \*\*\* $P < 0.001$ , \*\* $P < 0.01$ , \* $P < 0.05$ , – =  $P > 0.05$ .

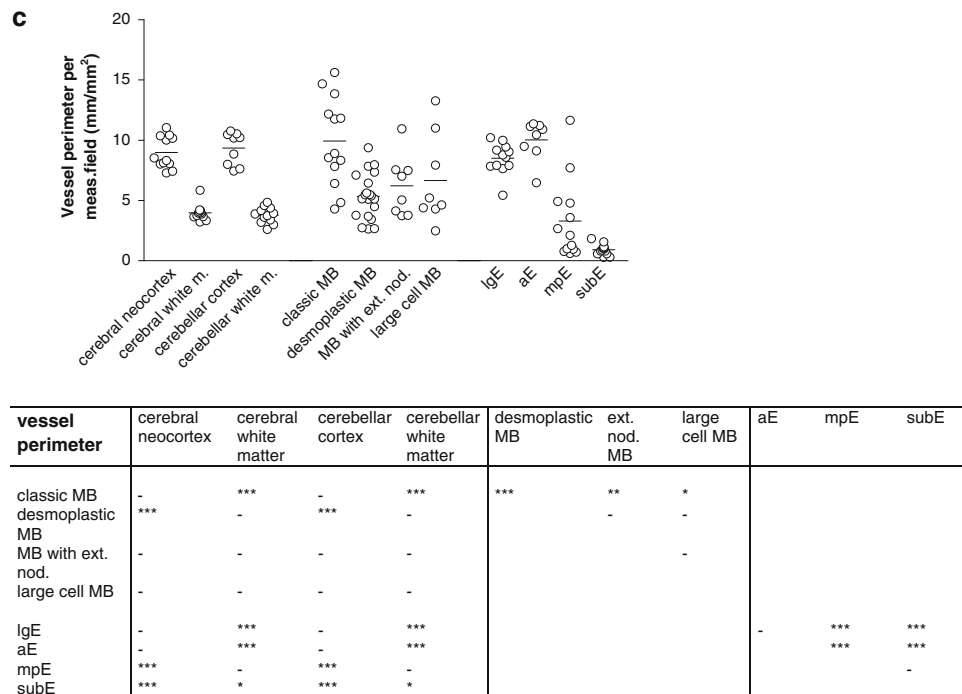


**Fig. 2** continued

avourable prognostic factor. This contrasts with another study of 78 children with MBs by Grotzer et al. [17], in which vessel density was not predictive of outcome. Nevertheless, these authors considered MBs as good candidates for anti-angiogenic strategies [17]. In a study of 112 cerebral ETs, progression-free survival time was found to be significantly shorter for VEGF and EGFR positive IgEs, as compared to VEGF and EGFR negative IgEs [14]. In another study of 100 intracranial ETs, markers for hypoxia (carbonic anhydrase 9, hypoxia-inducible factor 1 alpha and VEGF) were not related to outcome [18]. In a study of supratentorial primitive neuroectodermal tumours and MBs, the spatial organisation of tumour vessels was described to allow for differentiation between different prognostic subtypes [19].

Our study is the first on 3D reconstruction of microvasculature in MBs and ETs. We conducted this study with the hypothesis that the histopathology of different subtypes is reflected by a difference in the tumour microvasculature and compared the architecture of the tumour vessels with that of normal cerebral and cerebellar tissue. For MBs, classic and large cell MBs had a denser vasculature pattern than desmoplastic MB and MB with extensive nodularity. In the latter two MB types we found vessels to be organised around the nodular, reticulin-free zones. In fact, this is what one would expect knowing that the nodules in

these subtypes are classically described as reticulin-free “pale islands” while the wall of blood vessels does contain reticulin. The vasculature of ETs varied widely. The most dense pattern was seen in aE, while at the other end of the spectrum subE only showed few but regular vessels. The vasculature of ETs, only mean vessel area was larger for IgE, aE and mpE, as compared to normal cerebral and cerebellar tissue. Variation of vascular parameters was high for all ETs, except for subE. The subE had less vessels than normal cerebral tissue.

For several reasons, our present 3D and quantitative results should be interpreted with some caution. First, in the one representative tumour that was investigated in each category, only two microscopic areas were used for 3D reconstruction and 8–20 microscopic fields were used for quantitative analysis. One cannot expect that this study fully accounts for intra- and inter-tumoural heterogeneity. Furthermore, it is important to realise

that, dependent on the growth pattern of the (brain) tumour studied, the intra-tumoural vessels may be newly formed vessels, incorporated pre-existent vessels, or a combination of both [21]. Especially in infiltrative tumours like MBs, the majority of the tumour vessels may in fact be incorporated vessels, while in ETs (that generally show a more expansive growth pattern) the vast majority of the tumour vasculature may well be derived from neovascularisation, especially so in the subE which typically grows as a solid, exophytic tumour in the ventricular system. Whether brain tumours with vascular parameters within the range of normal cerebral and cerebellar tissue are good candidates for anti-angiogenic therapies depends on the actual degree of neovascularisation. Anti-angiogenic therapies are considered effective only if newly formed vessels are targeted [22, 23]. Even in the absence of newly formed vessels, however, microenvironmental factors may cause vascular changes like vasodilatation. In the quantitative part of our study the latter would result in (regions with) increased vessel area and perimeter without an increase in vessel number. For these reasons, a correlation based on the present study between angiogenesis and clinical behaviour can not be given. The clinical most aggressive histopathological MB subtype, large cell MB, did not have the largest number of vessels, or vessel perimeter. There was no statistically significant difference in number of vessels, vessel area, and vessel perimeter between aE and IgE. Interestingly, our quantitative analysis revealed a somewhat higher vessel number in normal cerebellar cortex than in normal cerebral neocortex. This finding might be explained by the fact that the areas selected for quantitative analysis of cerebellar cortex were all located in the granular layer. As this layer contains an extremely high number of (small) neurons, one can imagine that the demand for oxygen and nutrients (and therefore the vascular density) is especially high in this zone.

In conclusion, 3D reconstructions contribute to a better understanding of the true aspect of tumour vasculature [11]. We found a spectrum of patterns in the 3D reconstructions of the microvasculature in MB and ET subtypes, ranging from intensely to sparsely vascularised. Our results clearly show the disorganised and tortuous nature of the vasculature of some MB and ET subtypes, aspects that are more difficult to appreciate in two-dimensional sections or by quantitative analysis. In the future, 3D reconstruction of the tumour microvasculature in combination with markers identifying newly formed vessels will be of help to determine the degree of angiogenesis dependency of tumours. Unfortunately, unequivocal markers for such

newly formed tumour vessels are not yet available. In animal models, 3D reconstructions can also be used to monitor the effects of anti-angiogenic treatment and to test hypotheses concerning the pathobiological significance of different stimuli or inhibitors of this process.

## References

1. Roberts RO, Lynch CF, Jones MP, Hart MN (1991) Medulloblastoma: a population-based study of 532 cases. *J Neuropathol Exp Neurol* 50:134–144
2. Lannering B, Marky I, Nordborg C (1990) Brain tumors in childhood and adolescence in west Sweden 1970–1984. *Epidemiol Survival Cancer* 66:604–609
3. Kleihues P, Cavernee WK (eds) (2000) Tumors of the central nervous system. *Pathology and Genetics* (2nd edn). IARC Press, Lyon France
4. Lamont JM, McManamy CS, Pearson AD, Clifford SC, Ellison DW (2004) Combined histopathological and molecular cytogenetic stratification of medulloblastoma patients. *Clin Cancer Res* 10:5482–5493
5. Perry A (2002) Medulloblastomas with favorable versus unfavorable histology: how many small blue cell tumor types are there in the brain. *Adv Anat Pathol* 9:345–350
6. Brown HG, Kepner JL, Perlman EJ, Friedman HS, Strother DR, Duffner PK, Kun LE, Goldthwaite PT, Burger PC (2000) “Large cell/anaplastic” medulloblastomas: a pediatric oncology group study. *J Neuropathol Exp Neurol* 59:857–865
7. Lombardi D, Scheithauer BW, Meyer FB, Forbes GS, Shaw EG, Gibney DJ, Katzmann JA (1991) Symptomatic subependymoma: a clinicopathological and flow cytometric study. *J Neurosurg* 75:583–588
8. Neri D, Bicknell R (2005) Tumour vascular targeting. *Nat Rev Cancer* 5:436–446
9. Tozer GM, Kanthou C, Baguley BC (2005) Disrupting tumour blood vessels. *Nat Rev Cancer* 5:423–435
10. Fischer I, Gagner JP, Law M, Newcomb EW, Zagzag D (2005) Angiogenesis in gliomas: biology and molecular pathophysiology. *Brain Pathol* 15:297–310
11. Gijtenbeek JMM, Wesseling P, Maass C, Burgers L, van der Laak JAWM (2006) Three-dimensional visualization of microscopic structures: a new technique, applicable on archival material. *Angiogenesis* 8:297–305
12. van der Laak JAWM, Westphal JR, Schalkwijk LJ, Pahlplatz MM, Ruiter DJ, de Waal RM, de Wilde PC (1998) An improved procedure to quantify tumour vascularity using true colour image analysis Comparison with the manual hot-spot procedure in a human melanoma xenograft model. *J Pathol* 184:136–143
13. Chan AS, Leung SY, Wong MP, Yuen ST, Cheung N, Fan YW, Chung LP (1998) Expression of vascular endothelial growth factor and its receptors in the anaplastic progression of astrocytoma, oligodendroglioma, and ependymoma. *Am J Surg Pathol* 22:816–826
14. Korshunov A, Golanov A, Timirguz V (2002) Immunohistochemical markers for prognosis of ependymal neoplasms. *J Neurooncol* 58:255–270
15. Kranenburg O, Gebbink MFBG, Voest EE (2004) Stimulation of angiogenesis by Ras proteins. *Biochim Biophys Acta* 1654:23–37
16. Ozer E, Sarialioglu F, Cetingoz R, Yuceer N, Cakmakci H, Ozkal S, Olgun N, Uysal K, Corapcioglu F, Canda S (2004)

- Prognostic significance of anaplasia and angiogenesis in childhood medulloblastomas: a pediatric oncology group study. *Pathol Res Pract* 200:501–509
17. Grotzer MA, Wiewrodt R, Janss AJ, Zhao H, Cnaan A, Sutton LN, Rorke LB, Philips PC (2001) High microvessel density in primitive neuroectodermal brain tumors of childhood. *Neuropediatrics* 32:75–79
  18. Preusser M, Wolfsberger S, Haberler C, Breitschopf H, Czech T, Slave I, Harris AL, Acker T, Budka H, Hainfellner JA (2005) Vascularization and expression of hypoxia-related tissue factors in intracranial ependymoma and their impact on patient survival. *Acta Neuropathol* 109:211–216
  19. Goldbrunner RH, Pietsch T, Vince GH, Bernstein JJ, Wagner S, Hageman H, Selby DM, Krauss J, Soerensen N, Tonn J (1999) Different vascular patterns of medulloblastoma and supratentorial primitive neuroectodermal tumors. *Int J Dev Neurosci* 17:593–599
  20. Gilhuis HJ, van der Laak JAWM, Weseling P, Boerman RH, Beute G, Teepen JL, Grotenhuis JA, Kapelle AC (2004) Inverse correlation between genetic aberrations and malignancy grade in ependymal tumours. *J Neurooncol* 66:111–116
  21. Kahan H, Sklar EM, Post MJ, Bruce JH (1996) MR characteristics of histopathologic subtypes of spinal ependymoma. *AJNR Am J Neuroradiol* 17:143–150
  22. Weseling P, Ruiters DJ, Burger PC (1997) Angiogenesis in brain tumors; pathobiological and clinical aspects. *J Neurooncol* 32:253–265
  23. Weseling P, van der Laak JA, Link M, Teepen HL, Ruiters DJ (1998) Quantitative analysis of microvascular changes in diffuse astrocytic neoplasms with increasing grade of malignancy. *Hum Pathol* 29:352–358